

Structural and functional computational analysis of nicotine analogs as potential neuroprotective compounds in Parkinson disease



Gina Paola Becerra^{a,b}, Felipe Rojas-Rodríguez^a, David Ramírez^c, Alix E. Loaiza^d, Fabian Tobar-Tosse^e, Sol M. Mejía^{b,*}, Janneth González^{a,*}

^a Laboratorio de Bioquímica Computacional Estructural y Bioinformática, Facultad de Ciencias, Pontificia Universidad Javeriana, Bogotá, Colombia

^b Laboratorio de Química Computacional, Departamento de Química, Facultad de Ciencias, Pontificia Universidad Javeriana, Bogotá, Colombia

^c Instituto de Ciencias Biomédicas, Facultad de Ciencias de la Salud, Universidad Autónoma de Chile, El Llano Subercaseaux 2801-Piso 5, 8900000, Santiago, Chile

^d Laboratorio de Síntesis Orgánica, Departamento de Química, Facultad de Ciencias, Pontificia Universidad Javeriana, Bogotá, Colombia

^e Departamento de Ciencias Básicas de la Salud, Facultad de Ciencias de la Salud, Pontificia Universidad Javeriana Cali, Cali, Colombia

ARTICLE INFO

Keywords:

Nicotine analogs
DFT calculations
Natural Bond Orbitals
Molecular Orbitals
Neurodegenerative Diseases

ABSTRACT

As the mechanism of interaction between nicotinic receptors with nicotine analogs is not yet fully understood, information at molecular level obtained from computational calculations is needed. In this sense, this work is a computational study of eight nicotine analogs, all with pyrrolidine ring modifications over a nicotine-based backbone optimized with B3LYP-D3/aug-cc-pVDZ. A molecular characterization was performed focusing on geometrical parameters such as pseudo-rotation angles, atomic charges, HOMO and LUMO orbitals, reactivity indexes and intermolecular interactions. Three analogs, A2 (3-(1,3-dimethyl-4,5-dihydro-1H-pyrazol-5-yl) pyridine), A3 (3-(3-methyl-4,5-dihydro-1H-pyrazol-5-yl)pyridine) and A8 (5-methyl-3-(pyridine-3-yl)-4,5-dihydroisoxazole), were filtered suggesting putative neuroprotective activity taking into account different reactivity values, such as their lowest hardness: 2.37 eV (A8), 2.43 eV (A2) and 2.56 eV (A3), compared to the highest hardness value found: 2.71 eV for A5 (3-((2S,4R)-4-(fluoromethyl)-1-methylpyrrolidine-2-yl) pyridine), similar to the value of nicotine (2.70 eV). Additionally, molecular docking of all 8 nicotine analogs with the $\alpha 7$ nicotinic acetylcholine receptor ($\alpha 7$ nAChR) was performed. High values of interaction between the receptor and the three nicotine analogs were obtained: A3 (-7.1 kcal/mol), A2 (-6.9 kcal/mol) and A8 (-6.8 kcal/mol); whereas the affinity energy of nicotine was -6.4 kcal/mol. Leu116 and Trp145 are key residues in the binding site of $\alpha 7$ nAChR interacting with nicotine analogs. Therefore, based upon these results, possible application of these nicotine analogs as neuroprotective compounds and potential implication at the design of novel Parkinson's treatments is evidenced.

1. INTRODUCTION

Parkinson disease is a complex multifactorial disease characterized by progressive degeneration of nigrostriatal dopaminergic neurons leading to both motor and non-motor symptomatology (Hardy and Lees, 2005; Shadrina et al., 2010). Epidemiological studies have associated consumption of tobacco with a lower incidence of Parkinson's disease (PD) showing an inverse correlation between smoking and PD prevalence (Chen et al., 2010; Fratiglioni and Wang, 2000; Hernán et al., 2001; Thacker et al., 2007; Villafane et al., 2007). Clinical trials have showed positive results with chronic exposure over small populations (Itti et al., 2009; Ritz et al., 2007; Villafane et al., 2007).

Naturally, tobacco has high concentrations of the enantiomeric form of (S)-Nicotine also called L-Nicotine (Pogocki et al., 2007). Moreover, different pre-clinical studies in mice and cell lines have shown that nicotine and nicotinic acetylcholine receptors (nAChRs) agonists are able to protect neuronal cell populations against cell death mechanisms (Barreto et al., 2015; Ciobica et al., n.d.; Costa et al., 2001; Huang et al., 2009; Quik et al., 2012). The capability of nicotine-like compounds to reduce neural damage suggest their importance as neuroprotective agents (Barreto et al., 2015; Quik, 2004). Some of the main hypothesis associated with nicotine positive effect relies upon receptor interaction modulating MAO and CYP enzymes, mitochondrial complex modulation preventing oxidative stress, liberation of dopamine and

Abbreviations: $\alpha 7$, nAChR $\alpha 7$ nicotinic acetylcholine receptor; PD, Parkinson's disease; NBO, natural bond orbital; HOMO, highest occupied molecular orbital; LUMO, lowest unoccupied molecular orbital

* Corresponding authors.

E-mail addresses: sol.mejia@javeriana.edu.co (S.M. Mejía), janneth.gonzalez@javeriana.edu.co (J. González).

<https://doi.org/10.1016/j.compbiolchem.2020.107266>

Received 10 December 2019; Received in revised form 1 April 2020; Accepted 13 April 2020

Available online 21 April 2020

1476-9271/ © 2020 The Authors. Published by Elsevier Ltd. This is an open access article under the CC BY-NC-ND license (<http://creativecommons.org/licenses/by-nc-nd/4.0/>).

postsynaptic regulation of apoptosis by neurotrophic factor production (Quik, 2004; Quik and Kulak, 2002). Subsequent findings demonstrate that nicotine effect on oxidative stress and neuroprotection is linked to the therapeutic scheme and posology (Belluardo et al., 2000; Costa et al., 2001; Villafane et al., 2007). Transdermal administration of nicotine into Parkinson patients showed improvement over motor symptomatology (Fagerström et al., 1994; Ishikawa and Miyatake, 1993). Nevertheless, secondary effects associated with dependency, respiratory and cardiovascular damage diminish the pharmacological application of nicotine (Wang et al., 2012). In this sense, nicotine-like compounds such as nicotine analogs interacting with nAChRs have been proposed as putative Parkinson therapeutics reducing secondary effects associated with nicotine administration and classical dopaminergic replacement therapies (Matveeva et al., 2000; Wei et al., 2005).

Structurally, nAChRs are non-selective cation ionotropic receptor associated with the exchange of Na^+ , K^+ and Ca^{2+} (Dani, 2001; Hernández-Morales and García-Colunga, 2009). Also, nAChR possesses a quaternary structure characterized by a pentameric symmetrical arrangement of subunits around a central pore (Grutter and Changeux, 2001). Neuronal nAChR diversity derives from both from homomeric or heteromeric subtypes, with at least one α and one β subunits in the heteromeric variants (Dani, 2001; Gotti and Clementi, 2004; Grutter and Changeux, 2001; Quik and Kulak, 2002). In terms of subunit variety, twelve different nicotinic subunit variants, $\alpha 2 - \alpha 10$ and $\beta 2 - \beta 4$, assemble to compose the receptor with specific biophysical and pharmacological properties (Carnevale et al., 2007; Hernández-Morales and García-Colunga, 2009). Primary distributed in muscle and brain, the major diversity of nAChRs are located in the central nervous system (Carnevale et al., 2007). Only one muscle nAChR variant is located in the neuromuscular junction, composed by either $\alpha 1$, $\beta 1$, γ , and δ subunits in a 2:1:1:1 ratio or $\alpha 1$, $\beta 1$, δ , and ϵ subunits in a 2:1:1:1 ratio, varying between embryonic and adult, respectively (Kalamida et al., 2007; A. Yamane et al., 2001; Akira Yamane et al., 2002). Functionally, different studies have shown that nicotine exerts its effect by interacting with several nAChRs such as $\alpha 7$ and $\alpha 4 \beta 2$ (Quik and Kulak, 2002). Nicotine-like compounds interacting with $\alpha 7$ nAChRs lead to an increase of Ca^{2+} flow and activation of downstream signaling pathways such as ERK/MAPK, JAK2/STAT3, calmodulin, PI3K/AKT and CREB (Buckingham et al., 2009; Nakaso et al., 2008; Quik et al., 2012; Zhu et al., 2017). Specifically, PI3K/AKT has been associated with neuroprotection due to activation of survival genes such as Bcl-2 (Buckingham et al., 2009; Quik et al., 2015).

Development of novel neuroprotective therapies associated with nAChRs has mainly focused upon the study of receptor agonists to counteract Parkinson's disease motor and non-motor symptomatology. Interestingly, only the $\alpha 7$ subunit, from the homomeric subfamily II, can be found in the central nervous system possessing an essential role in neuroinflammation and neurodegeneration (Bencherif et al., 2011; Conejero-Goldberg et al., 2008; Gotti and Clementi, 2004; Quik et al., 2012). *In vitro* and *in vivo* evidence has shown that usage of nicotine-like compounds, in this case nicotine analogs, specifically interacting with $\alpha 7$ -nAChR, can reduce superoxide anion, hydrogen peroxide and oxidative stress levels (Jurado-Coronel et al., 2016). It is worth noticing that specificity of agonists is essential considering the side effects and dependency results from a non-selective activation of nAChR (Jurado-Coronel et al., 2016). Nicotine might act upon a diverse range of receptor subtypes producing a broad spectrum of behavioral effects, reducing its potential as pharmacological agent (Jurado-Coronel et al., 2016). Nevertheless, nicotine analogs with specific $\alpha 7$ -nAChR interaction, reduced secondary effects and neuroprotective activity are relevant in the PD pharmacological therapeutics.

Recent studies have shown that it is possible to develop selective nicotinic analogs with positive cognitive effects while avoiding addiction (Rezvani and Levin, 2001). Similarly, activation of nAChRs by nicotine, nicotine analogs or cotinine decreased neuroinflammation and stimulated synaptic plasticity in PD (Jurado-Coronel et al., 2016). All of

this has led to nicotine analogs becoming an active area of research to identify promising pharmacological agents for PD management (Quik, 2004; Zanardi et al., 2002). Recently, positive protective effects of the nicotine analogs (E)-nicotinaldehyde, O-cinnamyloxime, and 3-(pyridin-3-yl)-3a,4,5,6,7,7a-hexahydrobenzo[d]isoxazole on SH-SY5Y dopaminergic cell line have been reported, subjected to rotenone insult, through the modulation of ROS production (Jurado-Coronel et al., 2019). Additionally, nicotine analogs synthesis has focused on oxo, tio and seleno analogs (Jasiewicz et al., 2014a,b). Experimental studies have tested affinity and selectivity of nicotine-like compounds with nAChR through radioligand techniques using [^3H]-Nicotine and [^3H]-Cytisine showed high selectivity to $\alpha 4 \beta 2$ (Rao et al., 2008). Nicotine analog SIB-1508Y increments striatum dopamine liberation through selective activation of $\alpha 4 \beta 2$ but has no effect over motor symptomatology (Costa et al., 2001; Rao et al., 2008; The Parkinson Study Group, 2006). On the other hand, only chalcogen lactam nicotine analogs have been studied computationally so far (Jasiewicz et al., 2014a,b). Hence, information at a molecular level for most nicotine analogs, such as geometric, energetic, population data, and so on, is still required. This kind of information is important because it could improve drug discovery methods, considering it can filter big sets of compounds against known ligands, activating specific biological responses.

With this in mind, in order to understand the mechanisms of binding of nicotine analogs to the $\alpha 7$ -nAChR receptor, 8 synthetic nicotine analogs (with the pyrrolidine ring modified) were energy and geometrically characterized. That characterization consisted on pseudorotation angles, folding degrees, atomic charges, highest occupied molecular orbital (HOMO) and the lowest unoccupied molecular orbital (LUMO) as well as functional interaction with $\alpha 7$ -nAChR to improve drug screening in PD neuroprotection. This information would provide insight into the molecular features associated with nicotine analog activity and can suggest the druggable potential of certain nicotine analogs. However, further experimental studies about the decreased toxicity of these analogs due to their modification in the pyrrolidine ring are required.

2. COMPUTATIONAL DETAILS

2.1. Conformational search and reactivity analysis

Geometrical variants were comparatively studied across the 8 nicotine analogs (Ax, x = 1 – 8): A1 ((3R,5S)-1, methyl-5-(pyridine-3-yl) pyrrolidine-3-ol), A2 (3-(1,3-dimethyl-4,5-dihydro-1h-pyrazole-5-yl) pyridine), A3 (3-(3-methyl-4,5-dihydro-1h-pyrazole-5-yl) pyridine), A4 (3(((2S,4R)-1,4-dimethylpyrrolidine-2-yl))), A5 (3-((2S,4R)-4-(fluoromethyl)-1-methylpyrrolidine-2-yl) pyridine), A6 (3-((2S,4R)-4-methoxy-1-methylpyrrolidine-2-yl) pyridine), A7 (3-((2S,3S)-1,3-dimethylpyrrolidine-2-yl) pyridine) and A8 (5-methyl-3-(pyridine-3-yl)-4,5-dihydroisoxazole). Plane structures of both nicotine and nicotine analogs are shown in Fig. 1.

3D structures of the 9 compounds (nicotine and nicotine analogs) were manually generated using Avogadro version 1.2.0 (Hanwell et al., 2012). Energy minimization correcting atom type and chirality, as well as conformational optimization with systematic conformer search algorithm were performed using MMFF94 force field in Avogadro. Resulting geometrical conformers were used as initial structures for optimization and refinement of geometric and reactivity data using Gaussian09 (Frisch et al., 2016). Conformational sampling using several combinations of torsion angle constraints for each analog was performed. Groups of optimized conformers were categorized taking into account the following parameters: A) geometrical conformation of the pyrrolidine ring as the phase angle of the pseudorotation P (Eq. (1)), and the degree of folding τ_m (Eq. (2)); B) orientation of the functional group in the N5, and C) rotation of the pyridine-pyrrolidine bond χ , defined by H1-(C1-C1'-C2') (Fig. 1A).

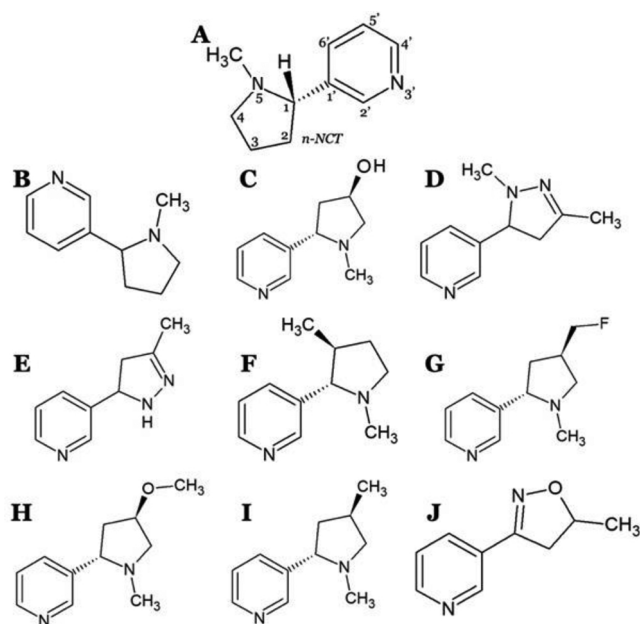


Fig. 1. Nicotine and nicotine analogs structure. A) Numeration of atoms across the nicotine backbone* B) Nicotine C) Nicotine Analogue 1 D) Nicotine Analogue 2 E) Nicotine Analogue 3 F) Nicotine Analogue 4 G) Nicotine Analogue 5 H) Nicotine Analogue 6 I) Nicotine Analogue 7 J) Nicotine Analogue 8. *Position numbers were preserved for analog atoms as well as radical indications.

$$\tan(P) = \frac{(V_4 + V_1) - (V_3 + V_6)}{2V_2(\sin 36^\circ + \sin 72^\circ)} \quad (1)$$

$$\tau m = \frac{V_2}{\cos P} \quad (2)$$

As already mentioned, resulting geometries were optimized and verified as true minima by frequency calculation employing the B3LYP functional including the D3 version of Grimme's dispersion with Becke-Johnson damping (Grimme et al., 2011) with the aug-cc-pVDZ basis set. This theoretical approach was chosen based on the study of tobacco alkaloids reported by Baranska et al. (2012) where good agreement between experimental and computational results were found. Population calculations were performed using the natural bond orbital (NBO) at the same theoretical approach using NBO program implemented on Gaussian 09. NBO analysis emphasizes the role of intermolecular orbital interaction in the complex, particularly charge transfer, performed by considering all possible interactions between filled donor and empty acceptor NBOs, as well as estimating their energetic importance by second-order perturbation theory. For each NBO donor (i) and NBO acceptor (j), the stabilization energy E is associated with electron delocalization between donor and acceptor.

Global reactivity indexes, besides local reactivity parameters were calculated, such as electronegativity (χ), hardness (η), softness (S) and electrophilicity (ω) using Eqs. (3) to (6), respectively, according to Koopmans' theorem which states that the first ionization energy (I) of a molecule is equal to the negative of the energy of the HOMO (Koopmans, 1934). In this sense, electron affinity is the negative of the energy of the LUMO. Specifically, electronegativity (χ), defined according to Mulliken's equation (Geerlings et al., 2003), is defined as shown in Eq. (3). Which means that electronegativity is equal to the negative value of the chemical potential (μ).

$$\chi = \frac{-(E_{HOMO} + E_{LUMO})}{2} = \frac{I + A}{2} \quad (3)$$

Hardness (η) is an index of global reactivity that allows to determine the resistance to electron redistribution in a system. In this sense, it is related to the difference in energy between the HOMO and LUMO

orbitals (Eq. (4)).

$$\eta = \frac{E_{LUMO} - E_{HOMO}}{2} \quad (4)$$

Softness (S) corresponds to the reciprocal of hardness, allowing to determine the tendency of a system to undergo changes in its electronic density and is defined by Eq. (5).

$$S = \frac{1}{2\eta} \quad (5)$$

Finally, electrophilicity (ω) is a global descriptor that allows to calculate the energetic stabilization of a system when electronic charge is acquired coming from the environment and calculated using Eq. (6).

$$\omega = \frac{\mu^2}{2\eta} \quad (6)$$

2.2. Docking simulations

In order to identify the interactions and specificity of nicotine analogs with $\alpha 7$ -nAChR, a molecular docking simulation of ligand-receptor interaction using the most stable conformer structure for each one of the analogs and nicotine was performed. For the receptor, $\alpha 7$ -nAChR crystallographic structure of the ligand binding domain was obtained from Protein Data Bank (PDB: 3SQ6). Considering that nAChR ligand binding pocket is located in the subunits interface (Grutter and Changeux, 2001), the active site located between chain A and B was used removing external ligands and solvation water molecules. $\alpha 7$ nAChR active site was identified based on experimental data of the receptor and interaction with epibatidine (Brejc et al., 2001; Grutter and Changeux, 2001; Li et al., 2011). Chains were explicitly minimized using NPT and NVP assembly and CHARMM force field implemented in GROMACS version 5.1.2 (Abraham et al., 2015).

Geometrically optimized analogs and nicotine as well as epibatidine were used for the protein-ligand complex simulation implemented in AutoDock 4 (Morris et al., 2009). The 3D structure of $\alpha 7$ nAChR in complex with epibatidine, a potent AChR agonist, was obtained from the same PDB structure 3SQ9. All the required file and format management was made using Autodock tools inner functions. Receptor was prepared adding polar hydrogens and nicotine, while nicotine analogs and epibatidine were kept rigid. Grid center coordinates were placed in the middle of the established, reported active site, so it focused on the coordinates: $x = 64,809$, $y = 46,396$, $z = 55,977$. Grid box dimensions (\AA) were 21, 17, and 16 in x , y , and z respectively. Ultimately, ten simulations for each ligand were made and the model with the lowest score of energy binding affinity score (kJ/mol) was selected.

3. RESULTS AND DISCUSSION

3.1. Geometry and Electronic Structure Analysis

Conformational searches provided 100 different (energy-minimized) topologies for each one of the nicotine analogs as well as nicotine. As previously described, conformers were ranked according to pseudorotation of the pyrrolidine ring (Eq. (1)), τm folding degree (Eq. (2)), functional group orientation and rotation of the pyridine-pyrrolidine bond (Eq. (3)). The majority of the low-energy structures have a similar topological arrangement characterized by the domains N ($-90^\circ \leq P < 18^\circ$), E ($18^\circ \leq P < 90^\circ$): χ for syn ($-170^\circ \leq \chi < -20^\circ$), Hsyn ($-20^\circ \leq \chi < 10^\circ$) and anti ($10^\circ \leq P < 160^\circ$). For the conformers categorization, the torsion angle for fluoromethyl group with respect to the pyrrolidine, defined by C3-C4-C7-F8, (C7) called $\chi 1$, was taken into account. According to the values of $\chi 1$, the following groups were defined: syn ($-180^\circ \leq \chi 1 < -150^\circ$), Hsyn ($-150^\circ \leq \chi 1 < 0^\circ$) y Hanti ($30^\circ \leq \chi 1 < 180^\circ$). Values energies, geometric and isomeric population parameters of the most stable conformers are presented in Table 1.

Table 1

Energy, geometric and population parameters of the most stable conformers for each nicotine analogs and nicotine. ^aRelative energies (kcal mol⁻¹), ^bPhase angle of Pseudorotación (°), ^cDegree of puckering(°), ^dBond piridyn-pyrrol(°), ^eFuntional group rotation and ^fIsomeric population

Conformation	ΔE^a	P^b	Tm^c	X^d	χ_1^e	IP^f
A1 E, trans, Hsyn	0,00	58,1	-1708,27	-19,66	-	65%
A2 E, trans, syn	0,00	71,1	38,56	-21,77	-	72%
A3 E, trans, anti	0,00	72,8	-18,81	25,24	-	74%
A4 E, trans, Hsyn	0,00	88,3	-2,86	-17,67	-	68%
A5 N, Hsyn, trans, syn	0,00	-89,4	7,53	64,66	-18,94	43%
A6 N, Hsyn, trans, Hsyn	0,00	73,0	62,17	-79,16	9,07	45%
A7 E, cis, anti	0,00	78,1	-18,89	114,34	-	60%
A8 N, trans, Hanti	0,00	-33,5	22,8	178,41	-	79%

No imaginary vibrational frequencies were found at the optimized geometries, indicating that they are true minima of the potential energy surface. From geometrical and energetic optimization calculations, 24 stable geometries classified in 8 groups were identified from the set of 144 original conformers. Most abundant (isomeric population) conformers structures were employed for further docking simulations, the 8 nicotine analog most stable and abundant from the 8 groups are displayed in Fig. 2.

Bond distances in different conformations can vary by up to 0.02 Å, and bond angles can vary by up to 11° with respect to nicotine. Nevertheless, analog 8 was an exception considering that the symmetrical form presented small deviations from the *piridyn-pyrrol* bond even though the equilibrium structure of the unperturbed (amide) group of the rings space is planar.

Atomic charges affect dipole moment, molecular polarizability,

electronic structure and some other properties of molecular systems. Formation of donor and acceptor pairs involving charge transfer in the molecule is suggested by charge distribution over the atoms (Table 2). Specific changes with respect to nicotine in the charge distribution of atoms present in the pyrrolidine ring were observed. Carbon atoms involved in the functionalization of analog 1 and analog 6 are acceptor centers presenting positive charge. Analogs 2 and 3 were characterized by the substitution of the C4 of the pyrrolidine ring by N (pyrazole), and analog 8 was characterized by the substitution of the C4 by an oxazole group. Substitutions of analogs 1, 2, 3, 6 and 8 resulted in atomic charges distribution changes of the heterocycle with respect to nicotine. Negative charge of C1 increases markedly compared with that presented in nicotine, turning these atoms into preferential centers of electrophilic attacks. Negative charge of C3 becomes positive, facilitating nucleophilic attack. Also, positive charge of C3 may also facilitate nucleophilic attacks in analog 2.

Frontier molecular orbitals comprising the HOMO and LUMO were calculated (Table 3), showing the same distribution pattern with respect to nicotine (Fig. 3). Notably, HOMO orbitals represent regions with electron donors while LUMO orbitals are associated with electron acceptor regions relevant to the global reactivity of the molecule. HOMO and LUMO orbitals were localized on the pyrrolidine and pyridine rings respectively, except for analog 3 in which the HOMO orbital was localized in both pyrrolidine and pyrrole ring (Fig. 3D). HOMO orbitals were distributed across the pyrrolidine ring, characterized by electron donor capacity or as a Lewis base, except for analog 8 where it was distributed across the pyridine ring (Fig. 3I). Analogs 2 and 3 HOMO orbitals were distributed across all the pyrrolidine ring, in contrast to the rest of the analogs where HOMO orbitals were distributed only over some of the pyrrolidine ring atoms. The atoms

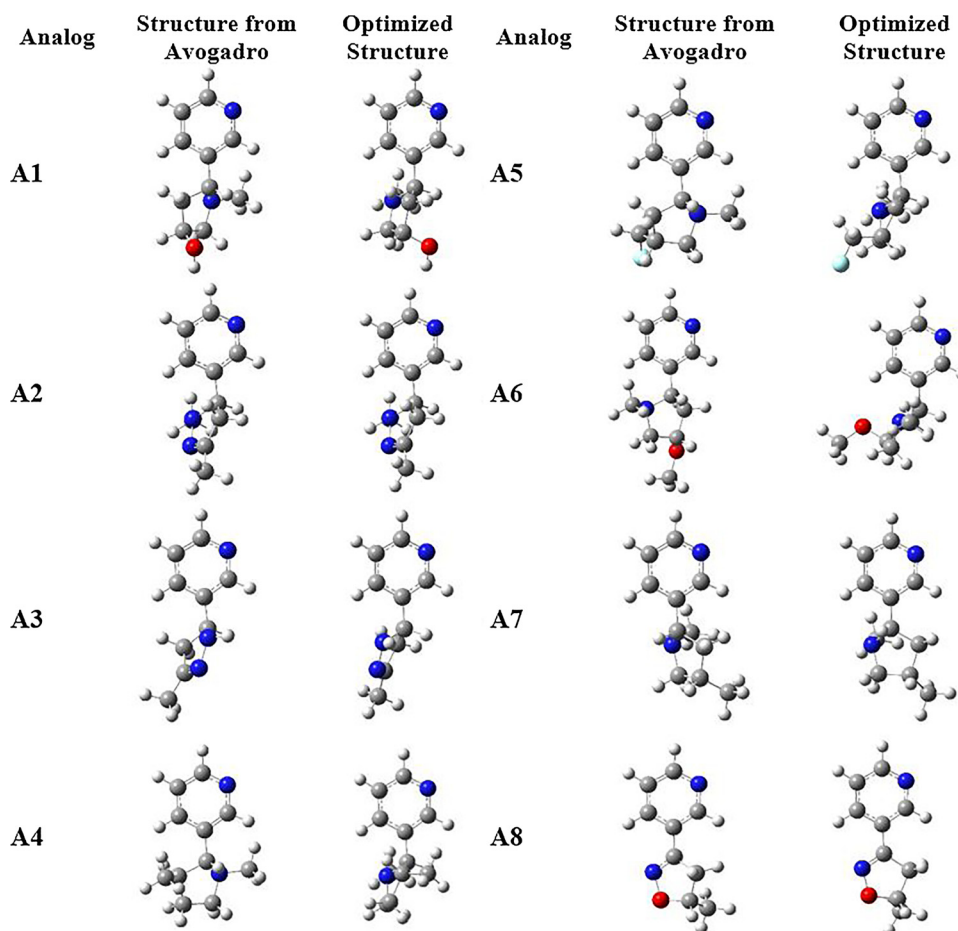


Fig. 2. Geometries of the eight nicotine analogs from the Avogadro program results and after the optimization in Gaussian program.

Table 2

NBO charges distributed across the pyrrolidine ring for both nicotine and nicotine analogs. Numeration of atoms corresponds to the pyrrolidine atoms for the analogs. Atom 6 correspond to the radical of the ring.

Atom number	Element	Nicotine	A1	A4	A5	A6	A7	Element	A2	A3	Element	A8
1	C	-0.040	-0.043	-0.041	-0.039	-0.040	-0.047	C	-0.051	-0.051	C	0.205
2	C	-0.422	-0.444	-0.231	-0.427	-0.448	-0.454	C	-0.478	-0.481	C	-0.512
3	C	-0.438	-0.124	-0.439	-0.294	0.114	-0.259	C	0.245	0.240	C	0.101
4	C	-0.208	-0.238	-0.210	-0.216	-0.239	-0.220	N	-0.286	-0.282	O	-0.400
5	N	-0.565	-0.574	-0.563	-0.568	-0.561	-0.565	N	-0.354	-0.510	N	-0.115
6	C	-0.408	-0.409	-0.413	-0.412	-0.409	-0.423	C	-0.699	-0.670	C	-0.667

Table 3

Reactivity parameters (in eV) of the most stable conformers. Energy of HOMO and LUMO, $GAP_{HOMO-LUMO}^a$, electronegativity^b, hardness^c, softness^d and electrophilicity^e

	E (HOMO)	E (LUMO)	GAP^a	χ^b	η^c	S^d	ω^e
A1	-5.90	-0.66	5.24	3.28	2.62	0.19	2.06
A2	-5.72	-0.86	4.86	3.29	2.43	0.21	2.22
A3	-5.95	-0.82	5.13	3.38	2.56	0.20	2.23
A4	-6.08	-0.73	5.35	3.41	2.68	0.19	2.02
A5	-6.27	-0.84	5.43	3.56	2.71	0.18	2.33
A6	-5.92	-0.59	5.33	3.25	2.67	0.19	1.99
A7	-5.90	-0.77	5.13	3.33	2.56	0.19	2.16
A8	-6.26	-1.51	4.75	3.88	2.37	0.21	3.17
Nicotine	-6.09	-0.69	5.40	3.39	2.70	0.19	2.13

without HOMO orbitals in the pyrrolidine ring were mainly the carbon with substitutions.

Frontier molecular orbitals comprising HOMO and LUMO were calculated (Table 3) showing the same distribution pattern with respect to nicotine (Fig. 3). HOMO and LUMO orbitals were localized on the pyrrolidine and pyridine rings respectively, except for analog 3 in which the HOMO orbital was localized in both pyrrolidine and pyrrole ring (Fig. 3D). Consequently, in general the pyrrole ring is the region of the molecule characterized by donor electron capacity or as a Lewis base. As expected, the LUMO orbitals of the analogs showed the same tendency with respect to nicotine being distributed over the pyridine ring, which indicated that this region of the molecule is characterized by its electron acceptor properties or Lewis acid character.

Global reactivity indexes are presented in Table 3. The chemical order of the nicotine analogs in terms of η (hardness) as follow: A8 > A2 > A3 > A7 > A1 > A6 > A4 > A5, with η indicating the resistance of the molecule to change their electron density distribution. In this sense, lowest value of η means a higher softness and electronegativity, suggesting analogs 2, 3 and 8 as the most reactive ones. Besides, A8 and A2 analogs present the smallest GAP HOMO-LUMO values indicating their highest reactivity among the compared nicotine analogs. Moreover, it is possible that higher reactivity of analogs 2, 3 and 8 favor the interaction with $\alpha 7$ -nAChR.

3.2. Binding interaction of nicotine analogs docked with $\alpha 7$ -nAChR

The $\alpha 7$ nAChR ligand binding site (Fig. 4A and 4B) is characterized by a large number of aromatic residues located at the interface of each of the two subunits. notably, the crystallographic structure used for all the analysis had a 64% sequence identity and 71% similarity with the native $\alpha 7$ receptor. In this regard, the values were expected considering the $\alpha 7$ nAChR structure used is a chimeric construct with a $\alpha 7$ extracellular domain (Fig. 4A). Residues of the active side are distributed across both subunits composed by residues of the A-C loops of the principal subunit and D-E loops of the complementary subunit. Specifically, the residues Tyr91 (Loop A), Trp145 (Loop B), Tyr184 and Tyr191 (Loop C), Trp53 (Loop D), and Leu106, Gln114 and Leu116 (Loop E) (Fig. 4B and Table 4) compose the $\alpha 7$ nAChR active pocket (Brejc et al., 2001; Grutter and Changeux, 2001; Li et al., 2011).

Considering that the active pocket is located in the contact interface of all the subunits, residues composing the binding site are distributed between the subunits: Tyr91, Trp145, Tyr184 and Tyr191 are located on one subunit (Fig. 4B - Blue) whereas Trp53, Leu106, Gln114 and Leu116 are located in the complementary subunit (Fig. 4B - Red). However, our results suggest that Thr146, Cys187, and Cys186 were also involved in ligand-receptor complex interaction of $\alpha 7$ nAChR with nicotine analogs (Table 4). Nicotine interacting at the interface of both subunits resulted in a geometrical conformational arrangement where the pyrrole ring is oriented towards the C-loop, favoring Van der Waals interactions with amino acids Tyr91, Trp145, and Tyr184 of the A chain (Fig. 4B Blue), in addition to Leu106 and Trp53 of the B chain (Fig. 4B Red). Moreover, the $\alpha 7$ nAChR binding site identified is in agreement with previous photo-affinity labeling and a mutagenesis studies (Barreto et al., 2015; Fratiglioni and Wang, 2000).

In terms of ligands interacting with the receptor, nicotine protonated ammonium was found to form a polar interaction with the delocalized electron and backbone carbonyl of Trp182. Values of interaction for epibatidine (-8,9 kcal/mol) showed a greater affinity in comparison to nicotine, therefore it was taken as a positive control. Our results showed that residues Tyr91, Trp145, Thr146, Tyr184 and Cys187 of chain A and Leu116 of chain B present Van der Waals interactions with epibatidine (Table 4). Additionally, for epibatidine, hydrogen bonds were identified between the carbonyl of the main chain of Trp145 and the nitrogen of the azabicyclo, the side chain of Leu116 and the amino group of pyridines and the side chain of Trp145 and the amino group of pyridine (Table 4). Both the Van der Waals interactions and the three hydrogen bonds are in concordance with previously reported interactions between epibatidine and $\alpha 7$ nAChR (Thompson et al., 2017). For affinity interaction in the ligand-receptor complex, analog 3 had a higher energy of interaction (-7.1 kcal/mol) in comparison to nicotine (-6.4 kcal/mol). Subsequently, it is suggested that the energy of interaction of analog 3 is associated with the ability of the pyridine ring to establish hydrogen bonds, particularly with Leu116 and Trp145 side chain, similarly to epibatidine. Our results show that A3 had a distance of 4.6 Å which is close to that reported for epibatidine (Abreo et al., 1996). Additionally, the pyridine ring of analog 3 forms hydrogen bonds with Leu116 main chain and Trp145 side chain like epibatidine does.

In this sense, epibatidine was used as a biological interaction standard for the novel nicotine analogs. Nevertheless, nicotine analogs with nicotine interactions were compared in order to elucidate a putative neuroprotective activity and correlation with the structural analysis. The residues interacting with the docked structures nicotine and nicotine analogs with the $\alpha 7$ nAChR active side are shown in Table 4. Accordingly, nicotine and analogs 2, 3, 4, 5, 6 and 8 were oriented towards the C loop in contrast to the E loop orientation of analogs 1 and 7. Orientations towards c loop favors the establishment of hydrogen bonds with pyridine in A3 and nicotine. These results are consistent with the predicted orientations suggesting that analog 3 is likely to occupy a similar location at nAChR $\alpha 7$ receptors compared with nicotine. Leu116 and Trp145 are essential for the high affinity of this type of analogs with $\alpha 7$ nAChR. This hypothesis is supported by the consistency between the docking result for epibatidine and previous

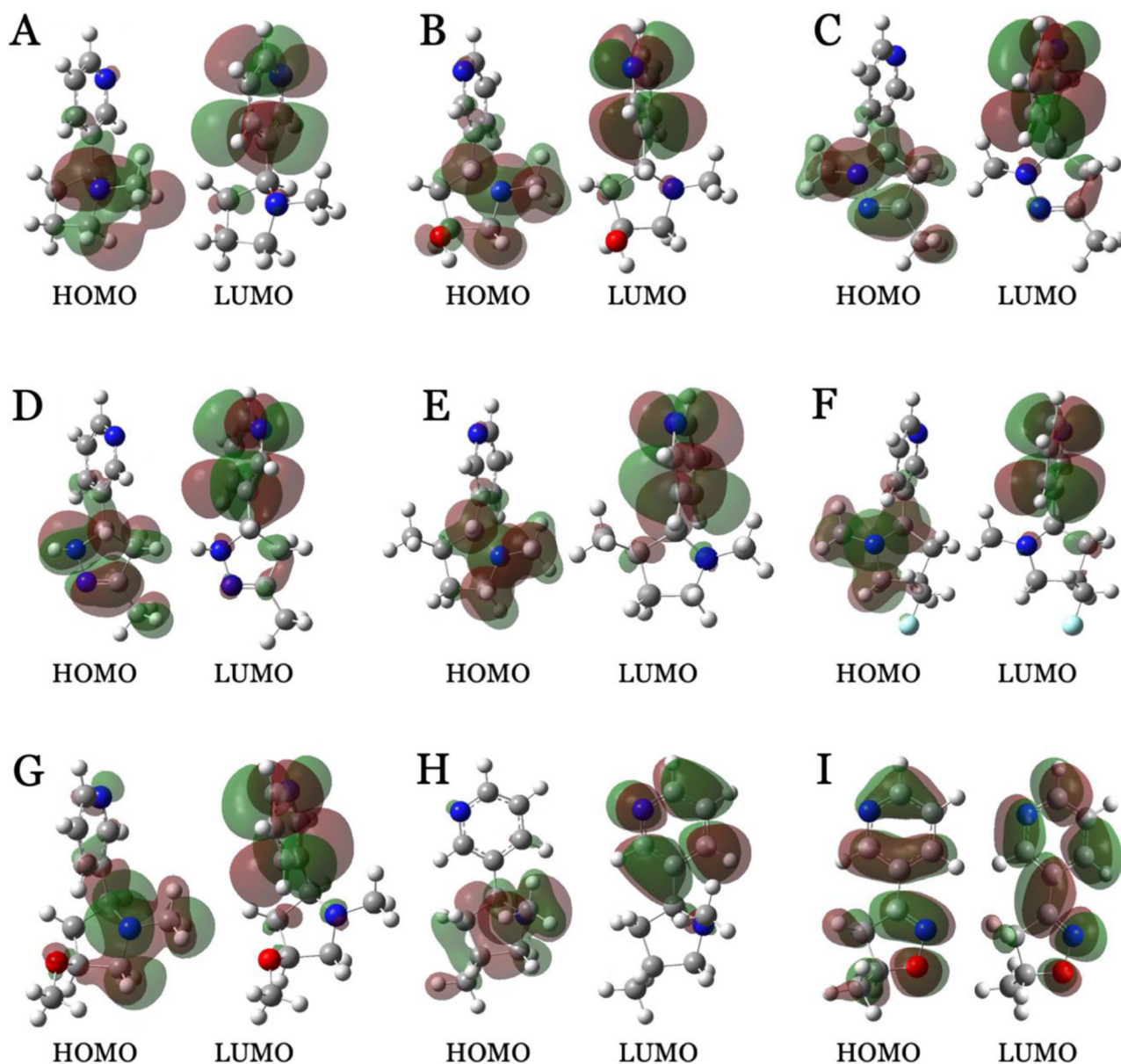


Fig. 3. HOMO and LUMO orbitals for nicotine and nicotine analogs. A) Nicotine B) Nicotine Analog 1 C) Nicotine Analog 2 D) Nicotine Analog 3 E) Nicotine Analog 4 F) Nicotine Analog 5 G) Nicotine Analog 6 H) Nicotine Analog 7 I) Nicotine Analog 8.

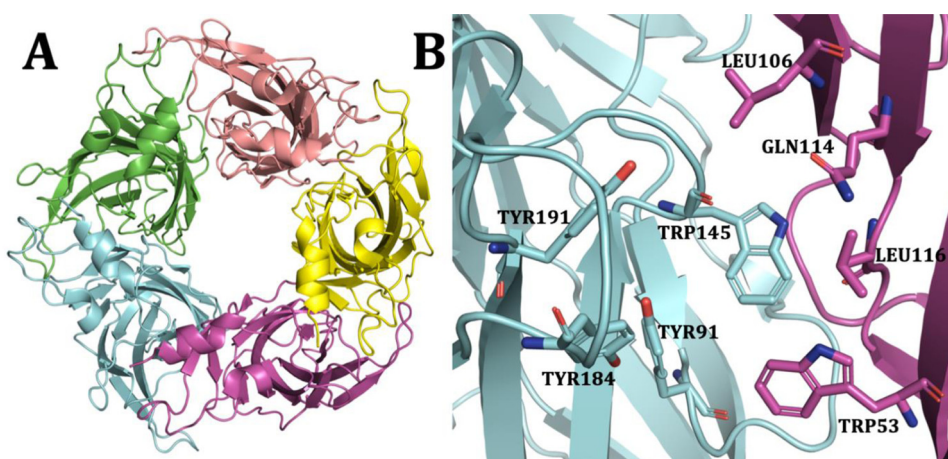


Fig. 4. Structure of the $\alpha 7$ nAChR extracellular domain (PDB 3SQ9) A) Pentameric structure of $\alpha 7$ nAChR. B) Residues present across one of the active pockets of the $\alpha 7$ nAChR. Blue residues are present in one of the subunits and red ones are from the complementary subunit.

Table 4

Molecular docking between nicotine, epibatidine and nicotine analogs with the active pocket of the $\alpha 7$ nAChR extracellular domain. Interactions and binding energies of affinity are presented. Discrimination between hydrogen bonds and hydrophobic interactions.

	Interactions		Energy of affinity (kcal/mol)
	Hydrophobic interactions	Hydrogen bonds	
Nicotine	CA: TYR191, TRP145, TYR184 CB: TRP53, LEU106	-	-6.4
Epibatidine	CA: TYR91, TRP145, Thr146, TYR184 and CYS187 CB: LEU116	TRP145, LEU116, TRP145	-8.9
A1	CA: THR146, TYR184, CYS187 CB: LEU106, LEU116	LEU116	-6.3
A2	CA: TYR91, TRP145, TYR184 CB: TRP53, LEU116	-	-6.9
A3	CA: TYR91, TRP145, TYR191 CB: LEU106, LEU116	LEU116, TRP145	-7.1
A4	CA: TYR91, TRP145, CYS186, CYS187, TYR191 CB: TRP53	-	-6.6
A5	CA: TYR91, TRP145, CYS187, TYR191 CB: TRP53, LEU106, LEU116	TRP145	-6.8
A6	CA: TYR91, TRP145, CYS186, TYR191 CB: TRP53, LEU116	-	-6.2
A7	CA: TRP145, THR146, CYS187 CB: TRP53, LEU106, LEU116	TRP53	-6.6
A8	CA: TYR91, TRP145 CB: LEU106, LEU116	LEU116	-6.8

computational studies (Li et al., 2011; Thompson et al., 2017). Steric effects were observed with C3 substituted analogs (dimethyl and fluoromethyl, analogs A2, A4, A5, and A7) decreasing the binding energy. In this sense, even though analog 2 was expected to have better interaction with the receptor suggested by low η values and high reactivity it could be discarded as a putative neuroprotective analog interacting with $\alpha 7$ nAChR. The deleterious effect could be due to steric occlusion in the receptor binding site, indicating that steric volume of a dimethyl group may represent a limit to geometrically match with the ligand binding domain. Such steric interaction appears to be more severe in the C3 substituted series than in the C5 substituted series, a phenomenon not observed with C4 substituted analogs (Table 4). Worthy of mention, C4 position configuration has a small effect on the geometrical matching.

In this sense, steric factors are fundamental for substituents optimal binding at the C3 position of the pyrrolidine ring. Further substitution with either an isoxazole or methyl causes less dramatic loss of affinity. Nevertheless, it is essential to experimentally test, both *in vitro* and *in vivo*, the potential neuroprotective activity of nicotine analogs. Accordingly, analogs 2, 3 and 8 were suggested as putative pharmacological agents in the context of PD neuroprotection based on the structural geometrical analysis. With the functional structural analysis of protein-ligand complex interaction with $\alpha 7$ nAChR, discrimination between the top three analogs considering steric effects was possible. Such process resulted in analog 2 discrimination considering protein-ligand complex interaction and energy of affinity. Therefore, both analogs, 3 and 8, represent the best neuroprotective candidates considering structural stability, reactivity and similarity with nicotine, as well as epibatidine-like interaction with $\alpha 7$ nAChR.

4. CONCLUSIONS

Results suggest that molecular characterizations focusing on geometric and reactivity parameters integrated with molecular docking is useful to improve screening of $\alpha 7$ nAChR agonists. Structurally, besides local indexes, global indexes of reactivity such as electronegativity (χ), hardness (η), softness (S) and electrophilicity (ω) allowed to filter three analogs with reactivity and HOMO and LUMO orbitals suggesting putative neuroprotective activity. Interaction between nicotine analogs showed that Leu116 and Trp145 amino acid residues are fundamental in the understanding of the high affinity of the analogs with $\alpha 7$ nAChR

extracellular domain. Conformational analysis and characterization based on geometric data and reactivity indexes showed that analogs 2, 3 and 8 are the most reactive ligands among the eight nicotine analogs studied. Nevertheless, analog 2 was discarded based on functional interaction and affinity with $\alpha 7$ nAChR. For analog 3, the oxazole function in C3 augmented receptor affinity similarly to epibatidine forming hydrogen bonds with Leu116 and Trp145. In this sense, analog 3 highlights as a promising neuroprotective molecule followed by analog 8. In summary, this study provides valuable information concerning the structural features of the pyrrolidine ring in nicotine and nicotine analogs. Also, potential effects of pyrrolidine ring substituents for the design of new $\alpha 7$ nAChR agonists were analyzed. However, further experimental validation is strongly recommended in order to address pharmacological parameters of new neuroprotective drugs, as well as characterize biological mechanisms associated with receptor response and signaling pathway activation.

Ethics approval and consent to participate

Not applicable.

Consent for publication

Not applicable.

Availability of data and material

Not applicable.

Funding

This study was supported by Pontificia Universidad Javeriana (Grant 6867 to JG).

Authors' contributions

GPB developed all the local indexes analysis as well as the molecular docking, DR and SM contributed to the global indexes analysis of nicotine analogs, FRR and JG contributed to the biological analysis of results as well as refining of the molecular docking. AEL provides the nicotine analog structures. Finally, all authors contributed to the

analysis of structural and biological data as well as manuscript writing and approval.

CRedit authorship contribution statement

Gina Paola Becerra: Conceptualization, Data curation, Formal analysis, Investigation, Methodology, Validation, Writing - original draft, Writing - review & editing. **Felipe Rojas-Rodríguez:** Data curation, Formal analysis, Methodology, Validation, Visualization, Writing - original draft, Writing - review & editing. **David Ramírez:** Data curation, Formal analysis, Methodology, Software, Writing - original draft, Writing - review & editing. **Alix E. Loaiza:** Conceptualization, Formal analysis, Investigation, Writing - original draft, Writing - review & editing. **Fabian Tobar-Tosse:** Conceptualization, Formal analysis, Investigation, Validation, Writing - original draft, Writing - review & editing. **Sol M. Mejía:** Conceptualization, Data curation, Formal analysis, Funding acquisition, Investigation, Methodology, Project administration, Software, Supervision, Writing - original draft, Writing - review & editing. **Janneth González:** Conceptualization, Data curation, Formal analysis, Funding acquisition, Investigation, Methodology, Project administration, Resources, Software, Supervision, Writing - original draft, Writing - review & editing.

Declaration of Competing Interest

The authors declare that they have no known competing financial interests or personal relationships that could have appeared to influence the work reported in this paper.

Acknowledgements

This work was supported by the Pontificia Universidad Javeriana, Bogotá, Colombia, grant ID 6867 to JG. D.R. thanks Conicyt—Programa de Cooperación Internacional grant No. REDES190074. We would like to thank to the Direction of Technology and Information support team at Pontificia Universidad Javeriana for the troubleshooting the server related issues.

References

- Abraham, M.J., Murtola, T., Schulz, R., Páll, S., Smith, J.C., Hess, B., Lindahl, E., 2015. GROMACS: High performance molecular simulations through multi-level parallelism from laptops to supercomputers. *SoftwareX* 1–2, 19–25. <https://doi.org/10.1016/j.softx.2015.06.001>.
- Abreo, M.A., Lin, N.H., Garvey, D.S., Gunn, D.E., Hettlinger, A.M., Wasicak, J.T., et al., 1996. Novel 3-pyridyl ethers with subnanomolar affinity for central neuronal nicotinic acetylcholine receptors. *Journal of Medicinal Chemistry* 39 (4), 817–825. <https://doi.org/10.1021/jm9506884>.
- Baranska, M., Dobrowolski, J.C., Kaczor, A., Chruszcz-Lipska, K., Gorz, K., Rygula, A., 2012. Tobacco alkaloids analyzed by Raman spectroscopy and DFT calculations. *Journal of Raman Spectroscopy* 43 (8), 1065–1073. <https://doi.org/10.1002/jrs.3127>.
- Barreto, G.E., Iarkov, A., Moran, V.E., 2015. Beneficial effects of nicotine, cotinine and its metabolites as potential agents for Parkinson's disease. *Frontiers in Aging Neuroscience* 6. <https://doi.org/10.3389/fnagi.2014.00340>.
- Belluardo, N., Mudò, G., Blum, M., Fuxe, K., 2000. Central nicotinic receptors, neurotrophic factors and neuroprotection. *Behavioural Brain Research* 113 (1–2), 21–34. [https://doi.org/10.1016/S0166-4328\(00\)00197-2](https://doi.org/10.1016/S0166-4328(00)00197-2).
- Bencherif, M., Lippiello, P.M., Lucas, R., Marrero, M.B., 2011. Alpha7 nicotinic receptors as novel therapeutic targets for inflammation-based diseases. *Cellular and Molecular Life Sciences* 68 (6), 931–949. <https://doi.org/10.1007/s00018-010-0525-1>.
- Brejč, K., van Dijk, W.J., Klaassen, R.V., Schuurmans, M., van der Oost, J., Smit, A.B., Sixma, T.K., 2001. Crystal structure of an ACh-binding protein reveals the ligand-binding domain of nicotinic receptors. *Nature* 411 (6835), 269–276. <https://doi.org/10.1038/35077011>.
- Buckingham, S.D., Jones, A.K., Brown, L.A., Sattelle, D.B., 2009. Nicotinic acetylcholine receptor signalling: Roles in Alzheimer's disease and amyloid neuroprotection. *Pharmacological Reviews* 61 (1), 39–61. <https://doi.org/10.1124/pr.108.000562>.
- Carnevale, D., Simone, R.D., Minghetti, L., 2007. Microglia-Neuron Interaction in Inflammatory and Degenerative Diseases: Role of Cholinergic and Noradrenergic Systems. *CNS & Neurological Disorders - Drug Targets* 6 (6), 388–397. <https://doi.org/10.2174/187152707783399193>.
- Chen, H., Huang, X., Guo, X., Mailman, R.B., Park, Y., Kamel, F., et al., 2010. Smoking duration, intensity, and risk of Parkinson disease. pp. 8.
- Ciobica, A., Padurariu, M., and Hritcu, L. (n.d.). The effects of short-term nicotine administration on behavioral and oxidative stress deficiencies induced in a rat model of Parkinson's disease. *Psychiatria Danubina*, 24(2), 12.
- Conejero-Goldberg, C., Davies, P., Ulloa, L., 2008. Alpha7 nicotinic acetylcholine receptor: A link between inflammation and neurodegeneration. *Neuroscience & Biobehavioral Reviews* 32 (4), 693–706. <https://doi.org/10.1016/j.neubiorev.2007.10.007>.
- Costa, G., Abin-Carrriquiry, J.A., Dajas, F., 2001. Nicotine prevents striatal dopamine loss produced by 6-hydroxydopamine lesion in the substantia nigra. *Brain Research* 7.
- Dani, J.A., 2001. Overview of nicotinic receptors and their roles in the central nervous system. *Biological Psychiatry* 49 (3), 166–174. [https://doi.org/10.1016/S0006-3223\(00\)01011-8](https://doi.org/10.1016/S0006-3223(00)01011-8).
- Fagerström, K.O., Pomerleau, O., Giordani, B., Stelson, F., 1994. Nicotine may relieve symptoms of Parkinson's disease. *Psychopharmacology* 116 (1), 117–119. <https://doi.org/10.1007/BF02244882>.
- Fratiglioni, L., Wang, H.-X., 2000. Smoking and Parkinson's and Alzheimer's disease: Review of the epidemiological studies. *Behavioural Brain Research* 113 (1–2), 117–120. [https://doi.org/10.1016/S0166-4328\(00\)00206-0](https://doi.org/10.1016/S0166-4328(00)00206-0).
- Frisch, M.J., Trucks, G.W., Schlegel, H.B., Scuseria, G.E., Robb, M.A., Cheeseman, J.R., et al., 2016. Gaussian 09 Revision D.01.
- Geerlings, P., De Proft, F., Langenaeker, W., 2003. Conceptual Density Functional Theory. *Chemical Review* 103 (5), 1793–1874. <https://doi.org/10.1021/cr990029p>.
- Grimme, S., Ehrlich, S., Goerigk, L., 2011. Effect of the damping function in dispersion corrected density functional theory. *Journal of Computational Chemistry* 32 (7), 1456–1465. <https://doi.org/10.1002/jcc.21759>.
- Gotti, C., Clementi, F., 2004. Neuronal nicotinic receptors: From structure to pathology. *Progress in Neurobiology* 74 (6), 363–396. <https://doi.org/10.1016/j.pneurobio.2004.09.006>.
- Grutter, T., Changeux, J.-P., 2001. Nicotinic receptors in wonderland. *Trends in Biochemical Sciences* 26 (8), 459–463. [https://doi.org/10.1016/S0968-0004\(01\)01921-1](https://doi.org/10.1016/S0968-0004(01)01921-1).
- Hanwell, M.D., Curtis, D.E., Lonie, D.C., Vandermeersch, T., Zurek, E., Hutchison, G.R., 2012. Avogadro: An advanced semantic chemical editor, visualization, and analysis platform. *Journal of Cheminformatics* 4 (1). <https://doi.org/10.1186/1758-2946-4-17>.
- Hardy, J., Lees, A.J., 2005. Parkinson's disease: A broken nosology. *Movement Disorders* 20 (S12), S2–S4. <https://doi.org/10.1002/mds.20532>.
- Hernán, M.A., Zhang, S.M., Rueda-DeCastro, A.M., Colditz, G.A., Speizer, F.E., Ascherio, A., 2001. Cigarette smoking and the incidence of Parkinson's disease in two prospective studies: Smoking and Parkinson's Disease. *Annals of Neurology* 50 (6), 780–786. <https://doi.org/10.1002/ana.10028>.
- Hernández-Morales, M., García-Colunga, J., 2009. Effects of nicotine on K⁺ currents and nicotinic receptors in astrocytes of the hippocampal CA1 region. *Neuropharmacology* 56 (6–7), 975–983. <https://doi.org/10.1016/j.neuropharm.2009.01.024>.
- Huang, L.Z., Parameswaran, N., Bordia, T., Michael McIntosh, J., Quik, M., 2009. Nicotine is neuroprotective when administered before but not after nigrostriatal damage in rats and monkeys. *Journal of Neurochemistry* 109 (3), 826–837. <https://doi.org/10.1111/j.1471-4159.2009.06011.x>.
- Ishikawa, A., Miyatake, T., 1993. Effects of smoking in patients with early-onset Parkinson's disease. *Journal of the Neurological Sciences* 117 (1–2), 28–32. [https://doi.org/10.1016/0022-510X\(93\)90150-W](https://doi.org/10.1016/0022-510X(93)90150-W).
- Itti, E., Villafane, G., Malek, Z., Brugières, P., Capacchione, D., Itti, L., et al., 2009. Dopamine transporter imaging under high-dose transdermal nicotine therapy in Parkinson's disease: An observational study. *Nuclear Medicine Communications* 30 (7), 513–518. <https://doi.org/10.1097/MNM.0b013e32832cc204>.
- Jasiewicz, B., Malczewska-Jaskóła, K., Kowalczyk, I., Warzajtis, B., Rychlewska, U., 2014a. Chalcone analogues of nicotine lactam studied by NMR, FTIR, DFT and X-ray methods. *Spectrochimica Acta Part A: Molecular and Biomolecular Spectroscopy* 128, 773–780. <https://doi.org/10.1016/j.saa.2014.02.158>.
- Jasiewicz, B., Mrówczyńska, L., Malczewska-Jaskóła, K., 2014b. Synthesis and haemolytic activity of novel salts made of nicotine alkaloids and bile acids. *Bioorganic & Medicinal Chemistry Letters* 24 (4), 1104–1107. <https://doi.org/10.1016/j.bmcl.2014.01.005>.
- Jurado-Coronel, J.C., Avila-Rodriguez, M., Capani, F., Gonzalez, J., Echeverria Moran, V., Barreto, G.E., 2016. Targeting the Nicotinic Acetylcholine Receptors (nAChRs) in Astrocytes as a Potential Therapeutic Target in Parkinson's Disease. *Current Pharmaceutical Design*. <https://doi.org/10.2174/138161282210160304112133>.
- Jurado-Coronel, J.C., Loaiza, A.E., Díaz, J.E., Cabezas, R., Ashraf, G.M., Sahebkar, A., et al., 2019. (E)-Nicotinaldehyde O-Cinnamylxime, a Nicotine Analog, Attenuates Neuronal Cells Death Against Rotenone-Induced Neurotoxicity. *Molecular Neurobiology* 56 (2), 1221–1232. <https://doi.org/10.1007/s12035-018-1163-0>.
- Kalamida, D., Poulas, K., Avramopoulou, V., Fostieri, E., Lagoumintzis, G., Lazaridis, K., et al., 2007. Muscle and neuronal nicotinic acetylcholine receptors: Structure, function and pathogenicity. *FEBS Journal* 274 (15), 3799–3845. <https://doi.org/10.1111/j.1742-4658.2007.05935.x>.
- Koopmans, T., 1934. Über die Zuordnung von Wellenfunktionen und Eigenwerten zu den Einzelnen Elektronen Eines Atoms. *Physica* 1 (1–6), 104–113. [https://doi.org/10.1016/S0031-8914\(34\)90011-2](https://doi.org/10.1016/S0031-8914(34)90011-2).
- Li, S.-X., Huang, S., Bren, N., Noridomi, K., Dellisanti, C.D., Sine, S.M., Chen, L., 2011. Ligand-binding domain of an $\alpha 7$ -nicotinic receptor chimera and its complex with agonist. *Nature Neuroscience* 14 (10), 1253–1259. <https://doi.org/10.1038/nn.2908>.
- Matveeva, E.D., Podrugina, T.A., Morozkin, I.G., Tkachenko, S.E., Zefirov, N.S., 2000. Synthesis and neuroprotective properties of isosteric analogs of nicotine. *Chemistry of Heterocyclic Compounds* 36 (10), 1149–1153.

- Morris, G.M., Huey, R., Lindstrom, W., Sanner, M.F., Belew, R.K., Goodsell, D.S., Olson, A.J., 2009. AutoDock4 and AutoDockTools4: Automated docking with selective receptor flexibility. *Journal of Computational Chemistry* 30 (16), 2785–2791. <https://doi.org/10.1002/jcc.21256>.
- Nakaso, K., Ito, S., Nakashima, K., 2008. Caffeine activates the PI3K/Akt pathway and prevents apoptotic cell death in a Parkinson's disease model of SH-SY5Y cells. *Neuroscience Letters* 432 (2), 146–150. <https://doi.org/10.1016/j.neulet.2007.12.034>.
- Pogocki, D., Ruman, T., Danilczuk, M., Celuch, M., Wałajtyś-Rode, E., 2007. Application of nicotine enantiomers, derivatives and analogues in therapy of neurodegenerative disorders. *European Journal of Pharmacology* 563 (1), 18–39. <https://doi.org/10.1016/j.ejphar.2007.02.038>.
- Quik, M., 2004. Smoking, nicotine and Parkinson's disease. *Trends in Neurosciences* 27 (9), 561–568. <https://doi.org/10.1016/j.tins.2004.06.008>.
- Quik, M., Kulak, J.M., 2002. Nicotine and Nicotinic Receptors; Relevance to Parkinson's Disease. *NeuroToxicology* 23 (4–5), 581–594. [https://doi.org/10.1016/S0161-813X\(02\)00036-0](https://doi.org/10.1016/S0161-813X(02)00036-0).
- Quik, M., Perez, X.A., Bordia, T., 2012. Nicotine as a potential neuroprotective agent for Parkinson's disease. *Movement Disorders: Official Journal of the Movement Disorder Society* 27 (8), 947–957. <https://doi.org/10.1002/mds.25028>.
- Quik, M., Zhang, D., McGregor, M., Bordia, T., 2015. Alpha7 nicotinic receptors as therapeutic targets for Parkinson's disease. *Biochemical Pharmacology* 97 (4), 399–407. <https://doi.org/10.1016/j.bcp.2015.06.014>.
- Rao, T.S., Adams, P.B., Correa, L.D., Santori, E.M., Sacca, A.I., Reid, R.T., Cosford, N.D.P., 2008. Pharmacological characterization of (S)-(2)-5-ethynyl-3-(1-methyl-2-pyrrolidinyl)pyridine HCl (SIB-1508Y, Altincline), a novel nicotinic acetylcholine receptor agonist. *Brain Research* 1234, 16–24. <https://doi.org/10.1016/j.brainres.2008.07.063>.
- Rezvani, A.H., Levin, E.D., 2001. Cognitive effects of nicotine. *Biological Psychiatry*. [https://doi.org/10.1016/S0006-3223\(00\)01094-5](https://doi.org/10.1016/S0006-3223(00)01094-5).
- Ritz, B., Ascherio, A., Checkoway, H., Marder, K.S., Nelson, L.M., Rocca, W.A., et al., 2007. Pooled Analysis of Tobacco Use and Risk of Parkinson Disease. *Archives of Neurology* 64 (7), 990. <https://doi.org/10.1001/archneur.64.7.990>.
- Shadrina, M.I., Slominsky, P.A., Limborska, S.A., 2010. Molecular Mechanisms of Pathogenesis of Parkinson's Disease. *International Review of Cell and Molecular Biology*, vol. 281. pp. 229–266. [https://doi.org/10.1016/S1937-6448\(10\)81006-8](https://doi.org/10.1016/S1937-6448(10)81006-8).
- Thacker, E.L., O'Reilly, E.J., Weisskopf, M.G., Chen, H., Schwarzschild, M.A., McCullough, M.L., et al., 2007. Temporal relationship between cigarette smoking and risk of Parkinson disease. *Neurology* 68 (10), 764–768. <https://doi.org/10.1212/01.wnl.0000256374.50227.4b>.
- The Parkinson Study Group, 2006. Randomized placebo-controlled study of the nicotinic agonist SIB-1508Y in Parkinson disease. *Neurology* 66 (3), 408–410. <https://doi.org/10.1212/01.wnl.0000196466.99381.5c>.
- Thompson, A.J., Metzger, S., Lochner, M., Ruepp, M.-D., 2017. The binding orientation of epibatidine at $\alpha 7$ nACh receptors. *Neuropharmacology* 116, 421–428. <https://doi.org/10.1016/j.neuropharm.2017.01.008>.
- Villafane, G., Cesaro, P., Rialland, A., Baloul, S., Azimi, S., Bourdet, C., et al., 2007. Chronic high dose transdermal nicotine in Parkinson's disease: An open trial: Chronic high dose transdermal nicotine in Parkinson's disease. *European Journal of Neurology* 14 (12), 1313–1316. <https://doi.org/10.1111/j.1468-1331.2007.01949.x>.
- Wang, J., Li, X., Yuan, Q., Ren, J., Huang, J., Zeng, B., 2012. Synthesis and Pharmacological Properties of 5-Alkyl Substituted Nicotine Analogs. *Chinese Journal of Chemistry* 30 (12), 2813–2818. <https://doi.org/10.1002/cjoc.201200952>.
- Wei, X., Sumithran, S.P., Deaciuc, A.G., Burton, H.R., Bush, L.P., Dvoskin, L.P., Crooks, P.A., 2005. Identification and synthesis of novel alkaloids from the root system of *Nicotiana tabacum*: Affinity for neuronal nicotinic acetylcholine receptors. *Life Sciences* 78 (5), 495–505. <https://doi.org/10.1016/j.lfs.2005.09.009>.
- Yamane, A., Ohnuki, Y., Saeki, Y., 2001. Developmental Changes in the Nicotinic Acetylcholine Receptor in Mouse Tongue Striated Muscle. *Journal of Dental Research* 80 (9), 1840–1844. <https://doi.org/10.1177/00220345010800091301>.
- Yamane, Akira, Saito, T., Nakagawa, Y., Ohnuki, Y., Saeki, Y., 2002. Changes in mRNA Expression of Nicotinic Acetylcholine Receptor Subunits during Embryonic Development of Mouse Masseter Muscle. *Zoological Science* 19 (2), 207–213. <https://doi.org/10.2108/zsj.19.207>.
- Zanardi, A., Leo, G., Biagini, G., Zoli, M., 2002. Nicotine and neurodegeneration in ageing. *Toxicology Letters* 127 (1–3), 207–215. [https://doi.org/10.1016/S0378-4274\(01\)00502-1](https://doi.org/10.1016/S0378-4274(01)00502-1).
- Zhu, Z., Wang, Y.-W., Ge, D.-H., Lu, M., Liu, W., Xiong, J., et al., 2017. Downregulation of DEC1 contributes to the neurotoxicity induced by MPP+ by suppressing PI3K/Akt/GSK3 β pathway. *CNS Neuroscience & Therapeutics* 23 (9), 736–747. <https://doi.org/10.1111/cns.12717>.